# Synthesis and Reactivity of Cyclopentadienylhafnium Phosphido Complexes. Hydrogenolysis and Carbon Monoxide Insertion for Hf-$PR_2$ Bonds†

**Dean M. Roddick, Bernard D. Santarsiero, and John E. Bercaw***

*Contribution No. 7097 from the Division of Chemistry and Chemical Engineering, California Institute of Technology, Pasadena, California 91125.* *Received October 12, 1984*

**Abstract:** The syntheses of mono(pentamethylcyclopentadienyl)hafnium derivatives with the bulky, soft donor ligand di(*tert*-butyl)phosphide $\{P(CMe_3)_2\}$ are described. $Cp^*HfCl_2\{P(CMe_3)_2\}$ (**1**) ($Cp^* = \eta^5$-$C_5Me_5$) and $Cp^*HfCl\{P(CMe_3)_2\}_2$ are obtained from $Cp^*HfCl_3$ and $LiP(CMe_3)_2$. Compound **1** reacts with neopentyllithium or benzylpotassium to afford $Cp^*HfCl(CH_2CMe_3)\{P(CMe_3)_2\}$ or $Cp^*HfCl(CH_2Ph)\{P(CMe_3)_2\}$, whereas $Cp^*HfMe_2\{P(CMe_3)_2\}$ and $Cp^*HfCl(Ph)\{P(CMe_3)_2\}$ are best prepared by treatment of $Cp^*HfMe_2Cl$ or $Cp^*HfPhCl_2$ with $LiP(CMe_3)_2$. $Cp^*HfMe_2\{P(CMe_3)_2\}$ reacts smoothly with $H_2$ to yield the surprisingly unreactive $[Cp^*HfMe(\mu\text{-}H)\{\mu\text{-}P(CMe_3)_2\}]_2$, whose X-ray determined structure ($a$ = 11.485 (2) Å, $b$ = 16.447 (5) Å, $c$ = 11.826 (2) Å, $\beta$ = 118.92 (1)°, $P2_1/c$) shows a quadruply bridged dimer (Hf-$CH_3$ = 2.258 (9) Å; Hf-P = 2.805 (2), 2.807 (2) Å; Hf-H = 2.12 (13), 2.33 (13) Å; Hf-ring centroid = 2.264 Å). The hafnium-phosphide bonds are also susceptible to hydrogenolysis. Thus, $Cp^*HfCl\{P(CMe_3)_2\}_2$ reacts rapidly with 2-3 atm of $H_2$ with the release of free $HP(CMe_3)_2$. The relative rates of hydrogenolysis of the Hf-R bond of $Cp^*HfCl(R)\{P(CMe_3)_2\}$ (R = $P(CMe_3)_2$, $CH_2CMe_3$, and $CH_2Ph$) suggest that the Hf-$P(CMe_3)_2$ bond energy is the weakest in the series. The similarity of Hf-$P(CMe_3)_2$ bond energies to those of hafnium alkyls is also evidenced by the rapid insertion of CO with **1** to generate the first carboxyphosphide derivative of a transition element, $Cp^*HfCl_2\{\eta^2\text{-}C(O)P(CMe_3)_2\}$, whose structure was determined ($a$ = 14.919 (2) Å, $b$ = 9.952 (1) Å, $c$ = 15.779 (2) Å, $P2_12_12_1$). The carboxyphosphide fragment shows some lengthening of the C—O bond, 1.284 (6) Å, and shortening of the P—C bond, 1.782 (5) Å, to suggest substantial contribution from P=C—O and P—C=O resonance forms (other important bond lengths: Hf—O 2.117 (4) Å; Hf—C(acyl) = 2.03 (5) Å; Hf—Cl = 2.383 (2), 2.393 (2) Å, Hf—ring centroid = 2.157 Å).

The chemistry of titanium, zirconium, and hafnium complexes with hard donor ligands such as chloride, alkoxide, and dialkylamide has been studied extensively.[1] In contrast, the chemistry of group 4 metals with soft donor ligands such as dialkylphosphide has been virtually ignored until recently. Prior to Baker's concerted efforts to explore the chemistry of early transition-metal phosphides,[2] only three examples of zirconium(IV) dialkylphosphide[3] and no hafnium(V) dialkylphosphide complexes had been reported.

Phosphide ligands are currently of interest in the field of bimetallic and cluster chemistry[4] because of their pronounced ability to form stable, bridged compounds. This stability is derived in part from the flexible nature of the ($\mu_2$-$PR_2$) linkages, which can accommodate a range of metal-metal bonding and nonbonding distances.[4a] On the other hand, Geoffroy and co-workers[5] have pointed out that in some cases, phosphide bridges are susceptible to coupling with alkyl, hydride, and carbene ligands, so that they may not be as chemically inert as had been generally believed. In mononuclear compounds, terminal phosphide ligands[2,6,7] may function as either one-electron or three-electron donor ligands, thus stabilizing coordinatively unsaturated complexes, while at the same time providing an incipient vacant coordination site.

In light of these considerations, we became interested in exploring the chemistry of hafnium(IV) dialkylphosphide complexes. Prior to this work, efforts[8] in our laboratory to prepare reactive zirconium hydrides via hydrogenolysis of $Cp^*ZrR_3$ ($Cp^* = \eta^5$-$C_5Me_5$; R = alkyl and phenyl) in the presence of free phosphine were unsuccessful, giving instead ill-defined insoluble, polymeric hydride-bridged products. By incorporation of the bulky dialkylphosphide ligand[9] $P(CMe_3)_2$ with intramolecular phosphine donor (M=$PR_2$) functionality, it was hoped that soluble hydride complexes could be obtained. We report herein the synthesis of mono- and bisphosphide complexes $Cp^*HfCl_2\{P(CMe_3)_2\}$ (**1**) and $Cp^*HfCl\{P(CMe_3)_2\}_2$ (**2**), as well as a number of monophosphide alkyl and aryl compounds derived therefrom. Hydrogenolysis of $Cp^*HfR_n\{P(CMe_3)_2\}_{3-n}$ proved to be a general reaction for cleavage of hafnium-alkyl bonds, yielding less soluble hydridophosphide dimers. The product from the reaction of $Cp^*Hf(CH_3)_2\{P(CMe_3)_2\}$ and $H_2$, $[Cp^*Hf(CH_3)(\mu\text{-}H)\{\mu\text{-}P(CMe_3)_2\}]_2$, has been structurally characterized. Moreover, the hafnium-phosphide bond of $Cp^*HfCl_2\{P(CMe_3)_2\}$ is also susceptible to hydrogenolysis affording $HP(CMe_3)_2$ and products derived from initially formed $Cp^*HfCl_2H$. $Cp^*HfCl_2\{P(CMe_3)_2\}$ is found to react readily with CO to give the novel, structurally characterized insertion product $Cp^*HfCl_2\{\eta^2\text{-}C(O)P(CMe_3)_2\}$.

## Results and Discussion

**1. Synthesis of Mono- and Bisphosphido Derivatives.** Treatment of $Cp^*HfCl_3$ with 1 equiv of $LiP(CMe_3)_2$ or excess $LiP(CMe_3)_2$ in diethyl ether afforded dark-green phosphide complexes

† In this paper the periodic group notation is in accord with recent actions by IUPAC and ACS nomenclature committees. A and B notation is eliminated because of wide confusion. Groups IA and IIA become groups 1 and 2. The d-transition elements comprise groups 3 through 12, and the p-block elements comprise groups 13 through 18. (Note that the former Roman number designation is preserved in the last digit of the new numbering: e.g., III → 3 and 13.)

(1) (a) Cardin, D. J.; Lappert, M. F.; Raston, C. L.; Riley, P. I. "Comprehensive Organometallic Chemistry"; Wilkinson, G., ed.; Pergamon Press: New York, 1982; Vol. 3, pp 559-634. (b) Wailes, P. C.; Coutts, R. S. P.; Weigold, H. "Organometallic Chemistry of Titanium, Zirconium and Hafnium"; Academic Press: New York, 1974. (c) Andersen, R. A. *Inorg. Chem.* **1979**, *18*, 2928. Andersen, R. A. *J. Organomet. Chem.* **1980**, *192*, 189. Planalp, R. P.; Andersen, R. A.; Zalkin, A. *Organometallics* **1983**, *2*, 16. (d) Hillhouse, G. L.; Bercaw, J. E. *Ibid.* **1982**, *1*, 1025.

(2) (a) Baker, R. T.; Whitney, J. F.; Wreford, S. S. *Organometallics* **1983**, 1049-1051. (b) Baker, R. T.; Krusic, P. J.; Tulip, T. H.; Calabrese, J. C.; Wreford, S. S. *J. Am. Chem. Soc.* **1983**, *105*, 6763-6765.

(3) (a) Ellerman, J.; Poersch, P. *Angew. Chem., Int. Ed. Engl.* **1967**, *6*, 355. (b) Stelzer, O.; Unger, E. *Chem. Ber.* **1977**, *110*, 3430. Johannsen, G.; Stelzer, O. *Ibid.* **1977**, *110*, 3438.

(4) (a) Jones, R. A.; Wright, T. L.; Atwood, J. L.; Hunter, W. E. *Organometallics* **1983**, *2*, 470. (b) Finke, R. G.; Ganghan, G.; Pierpont, C.; Cass, M. E. *J. Am. Chem. Soc.* **1981**, *103*, 1394. (c) Roberts, D. H.; Steinmetz, G. R.; Breen, M. J.; Shulman, P. M.; Morrison, E. D.; Duttera, M. R.; DeBrosse, C. W.; Whittle, R. R.; Geoffroy, G. L. *Organometallics* **1983**, *2*, 846 and references therein.

(5) Geoffroy, G. L.; Rosenberg, S.; Shulman, P. M.; Whittle, R. R. *J. Am. Chem. Soc.* **1984**, *106*, 1519-1521.

(6) (a) Domaille, P. J.; Foxman, B. M.; McNeese, T. J.; Wreford, S. S. *J. Am. Chem. Soc.* **1980**, *102*, 4114. (b) Rocklage, S. M.; Schrock, R. R.; Churchill, M. R.; Wasserman, H. J. *Organometallics* **1982**, *1*, 1332.

(7) Jones, R. A.; Lasch, J. G.; Norman, N. C.; Whittlesey, B. R.; Wright, T. C. *Organometallics* **1982**, *1*, 6184.

(8) Wolczanski, P. T.; Bercaw, J. E. *Organometallics* **1982**, *1*, 793.

(9) The steric influence of $P(CMe_3)_2$ in bridging metal systems has recently been investigated: Jones, R. A.; Stuart, A. L.; Atwood, J. L.; Hunter, W. E.; Rogers, R. D. *Organometallics* **1982**, *1*, 1721. *Ibid.* **1983**, *2*, 874. Atwood, J. L.; Hunter, W. E.; Jones, R. A. *Inorg. Chem.* **1983**, *22*, 993.

0002-7863/85/1507-4670$01.50/0 

**Table I.** NMR[a] Data

| compound | assignment | nucleus | chem shift | coupling, Hz |
|---|---|---|---|---|
| $Cp^*HfCl_2\{P(CMe_3)_2\}$ (**1**) | $C_5(CH_3)_5$ | $^1H$ | 2.10 (d) | $J_{PH}$ = 0.3 |
| | $P(C(CH_3)_3)_2$ | | 1.45 (d) | $J_{PH}$ = 12.2 |
| | $P(C(CH_3)_3)_2$ | $^{31}P\{^1H\}$ | 209.9 | |
| $Cp^*HfCl\{P(CMe_3)_2\}_2$ (**2**) | $C_5(CH_3)_5$ | $^1H$ | 2.19 (s) | |
| | $\{P(C(CH_3)_3)_2\}_2$ | | 1.59 (d) | $J_{PH}$ = 12.6 |
| | $\{P(C(CH_3)_3)_2\}_2$ | $^{31}P\{^1H\}$ | 261.3 | |
| $Cp^*HfCl(CH_2(CH_3)_3\{P(CMe_3)_2\}$ (**3**) | $C_5(CH_3)_5$ | $^1H$ | 2.05 (s) | |
| | $P(C(CH_3)_3$ | | 1.45 (d) | $J_{PH}$ = 12.9 |
| | $CH_2C(CH_3)_3$ | | 1.37 (s) | |
| | $CH_2C(CH_3)_3$ | $^{31}P\{^1H\}$ | −0.20 (d) | $J_{HH}$ = 13.5 |
| | $P(C(CH_3)_3)_2$ | | 213.6 | |
| $Cp^*HfCl(CH_2Ph)\{P(CMe_3)_2\}$ (**4**) | $C_5(CH_3)_5$ | $^1H$ | 2.00 (s) | |
| | $P(C(CH_3)_3)_2$ | | 1.30 (d) | $J_{PH}$ = 13.1 |
| | $CH_2C_6H_5$ | | 6.8–7.4 (m) | |
| | $CH_2C_6H_5$ | | 1.74 (dd) | $^2J_{HH}$ = 13.2, $^3J_{PH}$ = 3 |
| | $P(C(CH_3)_3)_2$ | $^{31}P\{^1H\}$ | 222.2 | |
| $Cp^*HfMe_2\{P(CMe_3)_2\}$ (**5**) | $C_5(CH_3)_5$ | $^1H$ | 1.98 (s) | |
| | $P(C(CH_3)_3)_2$ | | 1.41 (d) | $J_{PH}$ = 12.9 |
| | $Hf(CH_3)_2$ | | 0.26 (d) | $J_{PH}$ = 2.5 |
| | $P(C(CH_3)_3)_2$ | $^{31}P\{^1H\}$ | 202.5 | |
| $Cp^*HfCl(Ph)\{P(CMe_3)_2\}$ (**6**) | $C_5(CH_3)_5$ | $^1H$ | 2.07 (s) | |
| | $P(C(CH_3)_3)_2$ | | 1.38 (d) | $J_{PH}$ = 13.2 |
| | $C_6H_5$ | | 8.13 (m) | |
| | $C_6H_5$ | | 7.20 (m) | |
| | $P(C(CH_3)_3)_2$ | $^{31}P\{^1H\}$ | 216.2 | |
| $Cp^*HfMe(Et)\{P(CMe_3)_2\}$ (**8**) | $C_5(CH_3)_5$ | $^1H$ | 1.97 (s) | |
| | $P(C(CH_3)_3)_2$ | | 1.35 (d) | $J_{PH}$ = 12.6 |
| | $Hf(CH_3)$ | | 0.24 (s, br) | |
| | $Hf(CH_2CH_3)$ | | 0.39 (q) | $J_{HH}$ = 8.1 |
| | $Hf(CH_2CH_3)$ | | 2.03 (t) | $J_{HH}$ = 8.1 |
| $Cp^*HfCl_2(Et)(PMe_3)$ (**11**) | $C_5(CH_3)_5$ | $^1H$ | 2.00 (s) | |
| | $P(CH_3)_3$ | | 0.97 (d) | $J_{PH}$ = 5.0 |
| | $Hf(CH_2CH_2)$ | | 0.75 (q) | $J_{HH}$ = 7.5 |
| | $Hf(CH_2CH_3)$ | | 1.80 (t) | $J_{HH}$ = 7.5 |
| $Cp^*HfCl_2\{\eta^2\text{-}C(O)P(CMe_3)_2\}$ (**12**) | $C_5(CH_3)_5$ | $^1H$ | 2.01 (s) | |
| | $P(C(CH_3)_3)_2$ | | 1.30 (d) | $J_{PH}$ = 13.5 |
| $Cp^*HfCl_2\{\eta^2\text{-}^{13}C(O)P(CMe_3)_2\}$ | $C_5(CH_3)_5$ | $^{13}C\{^1H\}$ | 11.77 (s) | |
| | $C_5(CH_3)_5$ | | 122.45 (s) | |
| | $P(C(CH_3)_3)_2$ | | 31.10 (d) | $J_{PH}$ = 7.9 |
| | $P(C(CH_3)_3)_2$ | | 38.11 (d) | $J_{PH}$ = 11.9 |
| | $Hf^{13}C(O)$ | | 3.03 (d) | $J_{PH}$ = 101.5 |
| | $P(C(CH_3)_3)_2$ | $^{31}P\{^1H\}$ | 92.6 (d) | $J_{PH}$ = 101.5 |

[a] $^1H$ (90 MHz), $^{13}C$ (22.5 MHz), and $^{31}P$ (26.3 MHz) NMR spectra measured in benzene-$d_6$ at ambient temperatures. $^1H$ and $^{13}C$ chemical shifts are reported in $\delta$ relative to internal TMS or residual protons or carbons in solvent. $^{31}P$ chemical shifts are reported in $\delta$ relative to 85% $H_3PO_4$ external standard. Coupling constants are reported in hertz.

$Cp^*HfCl_2\{P(CMe_3)_2\}$ (**1**) and $Cp^*HfCl\{P(CMe_3)_2\}_2$ (**2**), respectively, in good yield (eq 1 and 2). Both **1** and **2** are highly

$$Cp^*HfCl_3 \xrightarrow{\text{1.0 equiv of } LiP(CMe_3)_2} \underset{\mathbf{1}}{Cp^*HfCl_2\{P(CMe_3)_2\}} \quad (1)$$

$$Cp^*HfCl_3 \xrightarrow{\text{excess } LiP(CMe_3)_2} \underset{\mathbf{2}}{Cp^*HfCl\{P(CMe_3)_2\}_2} \quad (2)$$

moisture-sensitive and lose $HP(CMe_3)_2$ rapidly upon exposure to air. Solution molecular weight ($C_6H_6$, calcd 529; found 512) as well as $^1H$ and $^{31}P$ NMR (see Table I) and analytical data support the formulation of **1** as a monomeric, terminal phosphide complex of the indicated stoichiometry. The $^{31}P\{^1H\}$ NMR spectra of **1** and **2** exhibit single low-field resonances at 209.9 and 261.3 ppm, respectively, and appear indicative of a $\pi$-donor, three-electron coordination mode for the phosphide ligands of **1** and **2**.[2] Significantly, both **1** and **2** exhibit $^1H$ NMR equivalent *tert*-butyl groups. The equivalence of *tert*-butyl groups in **1** is consistent with a static structure **A**, where the *tert*-butyl groups are related

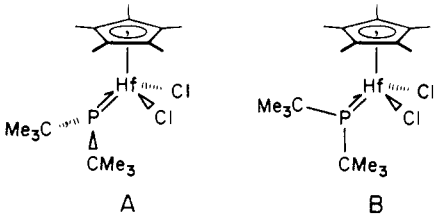


A B

by a mirror plane; however, the observation of a single resonance for *tert*-butyl groups for **2** and the asymmetrical alkyl derivatives (vide infra) requires equilibration via a fluxional process and suggests that rotation about the Hf–P bond in these complexes is rapid on the NMR time scale. Only slight broadening of the *tert*-butyl resonances (500 MHz) for **1** and **2** was observed down to −94 °C, placing an upper limit of ~10 kcal on $\Delta G^{\ddagger}$ for site exchange. Unfortunately, these observations do not allow a distinction to be made between A and B as the more stable, ground-state structure for **1**.

Preparative routes to a number of alkyl and aryl derivatives of **1** and **2** have been examined. Attempts to prepare methyl and phenyl derivatives of **1** by direct metathesis of $Cp^*HfCl_2\{P(CMe_3)_2\}$ with MeLi, MeMgBr, or PhLi at −78 °C were not successful. However, reaction of **1** with 1 equiv of $LiCH_2CMe_3$ in toluene or $KCH_2Ph$ in ether yielded 90% pure ($^1H$ NMR) $Cp^*HfCl(CH_2CMe_3)\{P(CMe_3)_2\}$ (**3**) and analytically pure $Cp^*HfCl(CH_2Ph)\{P(CMe_3)_2\}$ (**4**) as deeply maroon or violet crystalline solids (eq 3 and 4). The phosphides $Cp^*HfMe_2\{P$-

$$\underset{\mathbf{1}}{Cp^*HfCl_2\{P(CMe_3)_2\}} \xrightarrow{LiCH_2CMe_3} \underset{\mathbf{3}}{Cp^*HfCl(CH_2CMe_3)\{P(CMe_3)_2\}} \quad (3)$$

$$\underset{\mathbf{1}}{Cp^*HfCl_2\{P(CMe_3)_2\}} \xrightarrow{KCH_2Ph} \underset{\mathbf{4}}{Cp^*HfCl(CH_2Ph)\{P(CMe_3)_2\}} \quad (4)$$

Scheme I

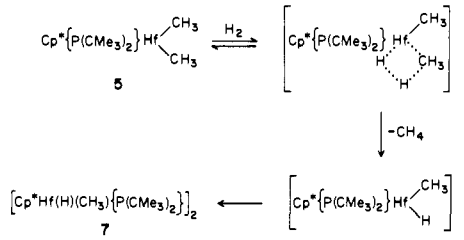

$(CMe_3)_2\}$ (**5**) and Cp*HfCl(Ph)$\{P(CMe_3)_2\}$ (**6**) may be readily obtained from the reaction of the corresponding chlorides $Cp^*HfMe_2Cl$ and $Cp^*HfPhCl_2$, prepared by metathesis of $Cp^*HfCl_3$ with MeMgBr or PhLi (see Experimental Section), with 1 equiv of $LiP(CMe_3)_2$ in diethyl ether (eq 5 and 6).

$$Cp^*HfMe_2Cl \xrightarrow{LiP(CMe_3)_2} Cp^*HfMe_2\{P(CMe_3)_2\} \quad (5)$$

$$Cp^*HfPhCl_2 \xrightarrow{LiP(CMe_3)_2} Cp^*HfCl(Ph)\{P(CMe_3)_2\} \quad (6)$$

Efforts to prepare alkyl derivatives of the sterically crowded bisphosphide **2** were unsuccessful. Neither treatment of **2** with MeLi or MeMgBr nor reaction of $Cp^*HfMeCl_2$ with excess $LiP(CMe_3)_2$ yielded any identifiable products.

All these phosphide derivatives are thermally quite stable and, like the parent dichloride **1**, are very soluble in aromatic, ethereal, and hydrocarbon solvents. $^{31}P\{^1H\}$ NMR resonances for **3–6** (200–225 ppm) are comparable to that observed for **1**, indicating similar terminal $\pi$-donor phosphide coordination.

**2. Reaction of $Cp^*_2HfMe_2\{P(CMe_3)_2\}$ (5) with Hydrogen.** A reaction which has been used with some success for preparation of various cyclopentadienyl hydrides of Zr[8,10] and Hf[10,11] is the hydrogenolysis of the corresponding methyl complex, as shown in eq 7. Therefore, in an attempt to generate $Cp^*HfH_2\{P(CMe_3)_2\}$, the reaction of dimethyl derivative **5** with $H_2$ was examined. Treatment of benzene solutions of **5** with 2–3 atm of $H_2$ at 25 °C induced clean loss of methane ($^1H$ NMR) over the course of several days to form an insoluble, crystalline yellow solid. Acidolysis of the isolated solid with HCl and Toepler analysis of the volatiles yielded 1.7 equiv of a 1:1 mixture of $H_2$ and $CH_4$ which, together with elemental analysis, indicates a product stoichiometry $[Cp^*Hf(H)Me\{P(CMe_3)_2\}]$ (**7**). The formulation

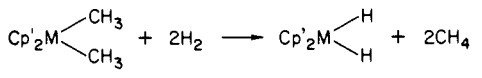

$$Cp'_2M(CH_3)_2 + 2H_2 \longrightarrow Cp'_2MH_2 + 2CH_4 \quad (7)$$

$$M = Zr, Hf$$

$$Cp' = C_5H_nMe_{4-n}R \quad (R = alkyl, H)$$

$$2Cp^*HfMe_2\{P(CMe_3)_2\} + 2H_2 \rightarrow [Cp^*Hf(H)Me\{P(CMe_3)_2\}]_2 + 2CH_4 \quad (8)$$

(5) (7)

of **7** as a dimer has been verified by its crystal structure (vide infra). Mass spectroscopic analysis of the methane produced in the reaction of **5** with $D_2$ indicated 95% $CH_3D$, consistent with a four-center hydrogenolysis mechanism[12,13] as shown in Scheme I.

The presence of hydride ligand in **7** has been confirmed by infrared spectroscopy ($\nu(Hf_2H_2)$ = 1510 $cm^{-1}$; $\nu(Hf_2D_2)$ = 1090 $cm^{-1}$; $\delta(Hf_2H_2)$ = 760 $cm^{-1}$; $\delta(Hf_2D_2)$ = 548 $cm^{-1}$). These IR data do not distinguish between terminal and bridging hydride-bonding modes.[14] Moreover, assignment of the structure of **7**

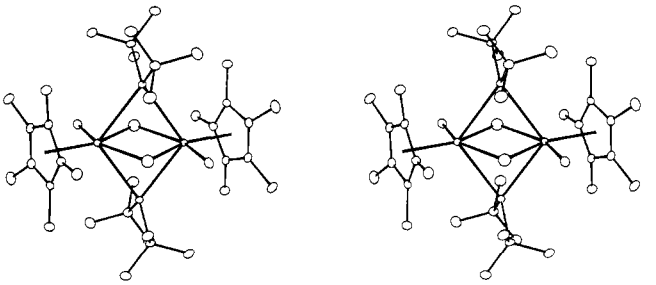

**Figure 1.** Stereoview of $[Cp^*HfMe(\mu\text{-}H)\{\mu\text{-}P(CMe_3)_2\}]_2$ (**7**).

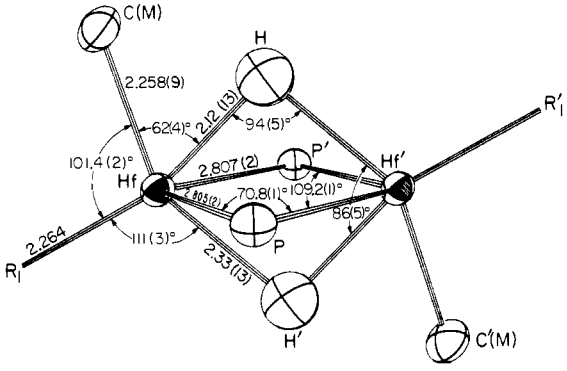


**Figure 2.** Skeletal view of $[Cp^*HfMe(\mu\text{-}H)\{\mu\text{-}P(CMe_3)_2\}]_2$ (**7**), with selected bond distances (Å) and angles (deg).

is further complicated by the ambidentate nature of the phosphine ligands, which may also adopt either terminal or bridging-bonding modes. Taken together, at least three possible dimeric structures may be envisioned. The structure of **7** has therefore been determined by X-ray diffraction.

**3. Structural Determination of $[Cp^*HfMe(\mu\text{-}H)\{\mu\text{-}P(CMe_3)_2\}]_2$ (7).** The molecular structure $[Cp^*HfMe(\mu\text{-}H)\{\mu\text{-}P(CMe_3)_2\}]_2$ (**7**) is presented as a stereoview in Figure 1, and a skeletal view of the immediate ligation about hafnium with relevant bond distances and bond angles is given in Figure 2. The molecular structure of **7** consists of two $(\eta^5\text{-}C_5Me_5HfMe(H)\{P(CMe_3)_2\}$ units bridged by two three-center, four-electron Hf–P–Hf bonds (Hf–P = 2.805 (2) Å, Hf–P′ = 2.807 (2) Å; P–Hf–P′ = 109.2 (1)°, Hf–P–Hf′ = 70.8 (1)°. The overall molecular symmetry of **7** is constrained by a crystallographic center of inversion located between hafnium atoms, resulting in a trans orientation of methyl and ring groups. The Hf–C(ring) distances range from 2.537 (9) to 2.589 (9) Å, closely similar to the average values of 2.54, 2.55 Å in $Cp^*_2Hf(H)(\eta^3\text{-}CH_2CHCH_2)$,[15] and somewhat longer than the average value of 2.47 Å for $Cp^*HfCl_2\{\eta^2\text{-}C(O)P(CMe_3)_2\}$ (vide infra). The Hf–C($\sigma$) bond length, 2.26 (1) Å, is intermediate between the reported values of 2.23 (1), 2.24 (1) Å in $Cp_2HfMe_2$,[16] 2.30 (1) Å in $[Cp_2HfMe]_2(\mu_2\text{-}O)$,[17] and 2.33(1) Å in $(\eta^5\text{-}C_9H_7)_2HfMe$.[18]

Details of the bonding of the hydride ligands in **7** are of primary interest, and although a precise determination of the coordinates of the hydride ligand was not possible, an examination of difference Fourier maps of the plane perpendicular to the $Hf_2P_2$ plane did reveal electron density attributable to the bridging hydride ligand. Subsequent least-squares refinement yielded the following pertinent information: Hf–H = 2.12 (13), 2.33 (13) Å, H–Hf–H′ = 86

(10) Couturier, S.; Gautheron, B. *J. Organomet. Chem.* **1978**, *157*, C61.
(11) Roddick, D. M.; Fryzuk, M. D.; Seidler, P. F.; Hillhouse, G. L.; Bercaw, J. E. *Organometallics*, in press.
(12) Gell, K. I.; Schwartz. *J. Am. Chem. Soc.* **1978**, *100*, 3246.
(13) Simpson, S. J.; Turner, H. W.; Andersen, R. A. *J. Am. Chem. Soc.* **1979**, *101*, 7728.
(14) Anomalously high-bridging hydride stretches have been noted for $[Cp_2TiH]_2$ (1450 $cm^{-1}$)[14a] and binuclear tantalum hydride complexes (1580–1600 $cm^{-1}$).[14b] (a) Bercaw, J. E.; Brintzinger, H. H. *J. Am. Chem. Soc.* **1969**, *91*, 7301. (b) Belmonte, P. A.; Schrock, R. R.; Day, C. S. *J. Am. Chem. Soc.* **1982**, *104*, 3082.
(15) Sanner, R. D.; Erwin, D. K.; Cohen, S. A.; Roddick, D. M.; Bercaw, J. E., unpublished results.
(16) Hunter, W. E.; Hrncir, D. C.; Vann Bynum, R.; Pentilla, S. A.; Atwood, J. L. *Organometallics* **1983**, *2*, 750.
(17) Fronzek, F. R.; Baker, E. C.; Sharp, P. R.; Raymond, K. N.; Alt, H. G.; Rausch, M. D. *Inorg. Chem.* **1976**, *15*, 2284.
(18) Atwood, J. L.; Hunter, W. E.; Hrncir, D. C.; Samuel, E.; Alt, H. G.; Rausch, M. D. *Inorg. Chem.* **1975**, *14*, 1757.

(5)°, and Hf–H–Hf′ = 94 (5)°. The observed asymmetry in the Hf–H bond lengths is not significant, but the average Hf–H bond length is reasonable for that of bridging hydride ligands, cf., 1.94 and 2.05 Å in $[(\eta^5\text{-}C_5H_4CH_3)_2ZrH(\mu\text{-}H)]_2$,[19] 2.069 (7) and 2.120 (8) Å in $(C_5H_4Me_2Hf(BH_4)_2$,[20] and 2.06 (2) Å and longer for terminal Hf–H bond lengths, cf., 1.78 (2) Å in $[(\eta^5\text{-}C_5H_5CH_3)_2ZrH(\mu\text{-}H)]_2$ and 1.85 (7) Å in $Cp^*{}_5Hf(H)(\eta^3\text{-}o\text{-}CH_2CHCH_2)$.[15,22] A further comparison of Hf–P bond lengths (average 2.806 Å) in **7** to reported terminal $\pi$-donor Hf–P values of $Cp_2Hf(PEt_2)_2$[2a] (2.488 Å) and $[Li(DME)][Hf(PCy_2)_5]$ (2.533, 2.475, and 2.504 Å) indicates that lengthening of the Hf–P bonds occurs upon bridging.

The general features of the structure are quite different than those of binuclear doubly bridged hydride complexes; the close H···P contacts, 2.59 and 2.90 Å, lead to short Hf···Hf′ and long H···H′ contacts when compared to the doubly bridged $[(\eta^5\text{-}C_5H_4CH_3)_2ZrH(\mu\text{-}H)]_2$ complex: Hf···Hf 3.25 vs. 3.46 Å for Zr···Zr, H···H 3.04 vs. 1.99 Å. It is evident from this structure that phosphide ligands do not provide a sufficiently sterically encumbering ligand environment for stabilization of monomeric hafnium hydride complexes. As a result, no significant steric interactions between the bulky *tert*-butylphosphide groups and the $(\eta^5\text{-}C_5Me_5)$ rings of **7** are incurred, and dimer formation is not prevented.

**4. Reactivity of $[Cp^*HfX(\mu\text{-}H)\{\mu\text{-}P(CMe_3)_2\}]_2$ (X = $CH_3$ and Cl).** $[Cp^*Hf(H)Me\{P(CMe_3)_2\}]_2$ (**7**) proved to be disappointingly inert. Unlike oligomeric $(Cp_2ZrH_2)_x$ or $(Cp_2Zr(H)Cl)_x$, which are sparingly soluble yet reactive in refluxing benzene, **7** is completely unreactive toward $H_2$, CO, or allene at room temperature. Upon heating to 80 °C, **7** decomposes both in the presence or absence of an excess of these substrates. $[Cp^*HfMe(\mu\text{-}H)\{\mu\text{-}P(CMe_3)_2\}]_2$ does, however, react slowly with excess ethylene at 25 °C to cleanly give ($^1$H NMR) the ethylene-inserted product, $Cp^*HfMe(Et)\{P(CMe_3)_2\}$ (**8**). Attempts to generate soluble, more

$$\underset{\mathbf{7}}{[Cp^*HfMe(\mu\text{-}H)\{\mu\text{-}P(CMe_3)_2\}]_2} \xrightarrow{C_2H_4} \underset{\mathbf{8}}{2Cp^*HfMe(Et)\{P(CMe_3)_2\}} \quad (9)$$

reactive, monomeric derivatives of **7** by cleavage of the formally 16-electron complex with donor ligands such as $PMe_3$ or $NMe_3$ were not successful. Another approach to the problem of enhancing reactivity of the hydride ligands is to increase the thermal stability of **7** by replacing the potentially reactive $CH_3$ group with Cl. Treatment of benzene solutions of $Cp^*HfCl(CH_2Ph)\{P(CMe_3)_2\}$ (**4**) or $Cp^*HfCl(CH_2CMe_3)\{P(CMe_3)_2\}$ (**3**) with $H_2$ readily afforded insoluble yellow **9**, formulated as the hydridochloride dimer $[Cp^*HfCl(\mu\text{-}H)\{\mu\text{-}P(CMe_3)_2\}]_2$ on the basis of a characteristic IR spectrum ($\nu(Hf_2H_2)$ = 1516 cm$^{-1}$; $\nu(Hf_2D_2)$ = 1085 cm$^{-1}$; $\delta(Hf_2H_2)$ = 770 cm$^{-1}$; $\delta(Hf_2D_2)$ = 540 cm$^{-1}$), analytical data, and by analogy to **7** (eq 10). Unfortunately, **9** proved no

$$\underset{\mathbf{3},\ R = CH_2CMe_3;\ \mathbf{4},\ R = CH_2Ph}{2Cp^*HfCl(R)\{P(CMe_3)_2\}} \xrightarrow[-RH]{H_2} \underset{\mathbf{9}}{[Cp^*HfCl(\mu\text{-}H)\{\mu\text{-}P(CMe_3)\}]_2} \quad (10)$$

more thermally stable than **7** and even less reactive, failing to insert $C_2H_4$ after prolonged exposure at 25 °C.

**5. Reactions of $Cp^*HfCl_2\{P(CMe_3)_2\}$ (1) and $Cp^*HfCl\{P(CMe_3)_2\}_2$ (2) with $H_2$.** During the course of investigating reactions of alkylphosphide complexes with $H_2$, it was found that hafnium–phosphide bonds are also susceptible to hydrogenolysis. The reaction of $Cp^*HfCl\{P(CMe_3)_2\}_2$ (**2**) with 2–3 atm of $H_2$ at 25 °C is rapid, quantitatively yielding **9** and 1 equiv of free phosphine, $HP(CMe_3)_2$. Qualitatively, for the series $Cp^*HfCl(R)\{P(CMe_3)_2\}$

$$\underset{\mathbf{2}}{Cp^*HfCl\{P(CMe_3)_2\}_2} + H_2 \rightarrow \underset{\mathbf{9}}{[Cp^*HfCl(\mu\text{-}H)\{\mu\text{-}P(CMe_3)_2\}]_2} + HP(CMe_3)_2 \quad (11)$$

(R = $P(CMe_3)_2$ (**2**), $CH_2CMe_3$ (**3**), and $CH_2Ph$ (**4**)), the observed relative rate of hydrogenolysis[25] is **2** > **3** ≫ **4**. Comparison of mean bond dissociation energies for the homoleptic alkyls $ZrR_4$ (R = $CH_2CMe_3$, $\bar{D}$ = 54 kcal mol$^{-1}$; R = $CH_2Ph$, $\bar{D}$ = 60 kcal mol$^{-1}$)[26] reveals the inverse order, so that the ease of hydrogenolysis of **2**, **3**, and **4** could correlate with the ligand bond strengths, with $D(Hf\text{–}CH_2Ph) > D(Hf\text{–}CH_2CMe_3) > D(Hf\text{–}P\{CMe_3\}_2)$ for this series. We hasten to add the caveat that reactivity commonly does not reflect the thermodynamic stability of a compound, so that the significance of this correlation is not yet clear.

The parent phosphide complex, $Cp^*HfCl_2\{P(CMe_3)_2\}$ (**1**), also reacts slowly with $H_2$ (3 atm) over the course of several weeks to give $HP(CMe_3)_2$ and disproportionation products $Cp^*HfCl_3$ and $(Cp^*HfH_2Cl)_x$,[27] plus 40% decomposition (eq 12). In the

$$\underset{\mathbf{1}}{Cp^*HfCl_2\{P(CMe_3)_2\}} \xrightarrow[-HP(CMe_3)_2]{H_2} \underset{\mathbf{10}}{[Cp^*HfCl_2H]} \rightarrow Cp^*HfCl_3 + (Cp^*HfH_2Cl)_x + \ldots \quad (12)$$

presence of 1 or more equiv of $PMe_3$, the hydrogenolysis of **1** is complete within minutes at 25 °C to give an uncharacterized mixture of products. The intermediacy of monohydride **10** in eq 12 is indicated, however, by trapping with excess ethylene to cleanly afford $Cp^*HfCl_2Et$. In the presence of excess $PMe_3$, the hydrogenolysis of **1** is complete within minutes at 25 °C to give an uncharacterized mixture of products. The intermediacy of monohydride **10** in eq 12 is indicated, however, by trapping with excess ethylene to cleanly afford $Cp^*HfCl_2Et$. In the presence of excess $PMe_3$, the reaction of **1** with 3 atm of $H_2$ and excess $C_2H_4$ is rapid, producing $HP(CMe_3)_2$ and $Cp^*HfCl_2Et(PMe_3)$ (**11**) quantitatively ($^1$H NMR). Compound **11** is isolated in 71% yield as an off-white analytically pure crystalline solid (eq 13).

$$\underset{\mathbf{1}}{Cp^*HfCl_2\{P(CMe_3)_2\}} + C_2H_4 + PMe_3 \xrightarrow{H_2} \underset{\mathbf{11}}{Cp^*HfCl_2Et(PMe_3)} + HP(CMe_3)_2 \quad (13)$$

**Scheme II**

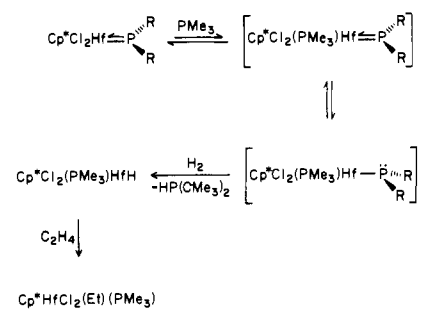


(19) Jones, S. B.; Petersen, J. L. *Inorg. Chem.* **1981**, *20*, 2889.
(20) Johnson, P. L.; Cohen, S. A.; Marks, T. J.; Williams, J. M. *J. Am. Chem. Soc.* **1978**, *100*, 2709.
(21) Broach, R. W.; I-ssuer Chuang; Marks, T. J.; Williams, J. M. *Inorg. Chem.* **1983**, *22*, 1081–1084.
(22) The ~0.35-Å difference between bridging and terminal hydride bond lengths for **7** and $Cp^*{}_2Hf(H)(\eta^3\text{-}CH_2CHCH_2)$ is higher than the 0.1–0.2-Å difference normally observed (Bau, R.; Carroll, W. E.; Teller, R. G.; Koetzle, T. F. *J. Am. Chem. Soc.* **1977**, *99*, 3872).
(23) This ~0.3-Å lengthening going from terminal to $\mu$-$PP_2$ coordination contrasts markedly with terminal and bridging Mo–P values for $Mo_2\{P(CMe_3)_2\}\{\mu\text{-}P(CMe_3)_2\}$ (Mo–P(terminal) = 2.382 (1) Å, Mo–P(bridge) = 2.437 (1), 2.434 (1) Å), which differ by only 0.06 Å (Jones, R. A.; Lasch, J. G.; Norman, N. C.; Whittlesey, B. R.; Wright, T. C. *J. Am. Chem. Soc.* **1983**, *105*, 6184).
(24) Closest intramolecular nonbonding C–H contacts are C(PB2)–H(22), C(PB3)–H(22) = 2.71 Å.
(25) Defining $t_{1/2}$ as the time at which the $P(CMe_3)_2$ resonance is half the integral value at $t$ = 0, at 25 °C, ~3 atm of $H_2$, $t_{1/2} \approx$ 5 min (**2**), 13 min (**3**), 7 h (**4**).
(26) Lappert, M. F.; Patil, D. S.; Pedley, J. B. *J. Chem. Soc., Chem. Commun.* **1975**, 830.
(27) Tentatively identified by $^1$H NMR.

Table II. IR and $^{13}C\{^1H\}$ NMR Data of M–($\eta^2$-C(O)R) Complexes

| compound | IR, $cm^{-1}$ | acyl $^{13}C$ chem shift, ppm | ref |
|---|---|---|---|
| $Cp^*_2ThCl(\eta^2\text{-}C(O)CH_2CMe_3)$ | 1469 | 360.2 | 29 |
| $c\text{-}Cp_2ZnMe(\eta^2\text{-}C(O)Me)^a$ | 1545 | | 30 |
| $l\text{-}Cp_2Zr(p\text{-tolyl})(\eta^2\text{-}C(O)(p\text{-tolyl}))$ | 1480 | 300 | 31 |
| $c\text{-}Cp_2Zr(p\text{-tolyl})(\eta^2\text{-}C(O)(p\text{-tolyl}))$ | 1505 | 301 | 31 |
| $Cp_2ZrCl(\eta^2\text{-}C(O)CH_2CMe_3)$ | 1550 | 318.7 | 32 |
| $Cp^*_2ThCl(\eta^2\text{-}C(O)NEt_2)$ | 1516 | 248.5 | 33 |
| $Cp_3U(\eta^2\text{-}C(O)CHPMePh_2)$ | 1440 | | 34 |
| $l\text{-}Cp^*_2ZrH(\eta^2\text{-}C(O)CHPMe_3)$ | 1427 | 250.3 | 35 |
| $c\text{-}Cp^*_2ZrH(\eta^2\text{-}C(O)CHPMe_3)$ | 1417 | 247.1 | 35 |
| $Cp^*HfCl_2\{\eta^2\text{-}C(O)P(CMe_3)_2\}$ (**12**) | 1350 | 3.03 | this work |

[a] *l* refers to the isomeric form where the acyl oxygen occupies the lateral equatorial site. *c* refers to the centrally located acyl oxygen isomer.

Whereas the origin of the phosphine promoter effect in reactions of **1** with $H_2$ is not fully understood, it should be noted that no significant effect by added $PMe_3$ on the rate of hydrogenolysis of the alkyl ligand in $Cp^*HfMeCl_2$ is observed. Thus, the phosphine effect on the rate of hydrogenolysis may be attributed to the loss of the $\pi$-donor interaction of the terminal phosphide with the metal center: coordination of phosphine of **1** in a rapid, albeit unfavorable equilibrium[28] to form a relatively electron-rich, 16-electron complex may weaken the phosphide lone-pair interaction with the hafnium, facilitating cleavage of the remaining $\delta$ bond by $H_2$ (Scheme II). Moreover, localization of the lone pair on phosphorus would be expected to enhance the rate of a heterolytic, four-center mechanism involving a polar transition state. This proposal may also be invoked to rationalize the

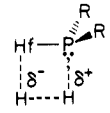


observed rapid hydrogenolysis of the bisphosphide complex **2** which is also formally a 16-electron complex.

**6. Synthesis and Structure of $Cp^*HfCl_2\{\eta^2\text{-}C(O)P(CMe_3)_2\}$ (12).** The results of the preceding section suggest that hafnium–phosphide bonds are comparable in strength to hafnium–alkyl bonds. Since group 4 alkyl complexes react readily with CO to give stable $\eta^2$-acyl products, it was anticipated that hafnium phosphide complexes would exhibit similar reactivity. Indeed, $Cp^*HfCl_2\{P(CMe_3)_2\}$ (**1**) reacts with 2 atm of CO at 25 °C within minutes to afford quantitatively ($^1H$ NMR) the carboxyphosphide insertion product $Cp^*HfCl_2\{\eta^2\text{-}C(O)P(CMe_3)_2\}$ (**12**) (eq 14).

$$Cp^*HfCl_2\{P(CMe_3)_2\} \xrightarrow{CO} Cp^*HfCl_2\{\eta^2\text{-}C(O)P(CMe_3)_2\} \quad (14)$$
**1** **12**

Compound **12**, isolated as a bright-yellow analytically pure crystalline solid (73%), exhibits a strong $\nu$(CO) band at 1350 $cm^{-1}$ which shifts to 1320 $cm^{-1}$ upon isotopic substitution with $^{13}CO$. This value is markedly lower than $\nu$(CO) values reported for related transition-metal and actinide $\eta^2$-acyl and $\eta^2$-carboxyamide complexes (see Table II) and is more comparable to values reported for exo and endo isomers of $Cp^*_2ZrH(\eta^2\text{-}C(O)CHPMe_3)$ ($\nu$(C–O) = 1427, 1417 $cm^{-1}$, respectively)[34,35] in which significant

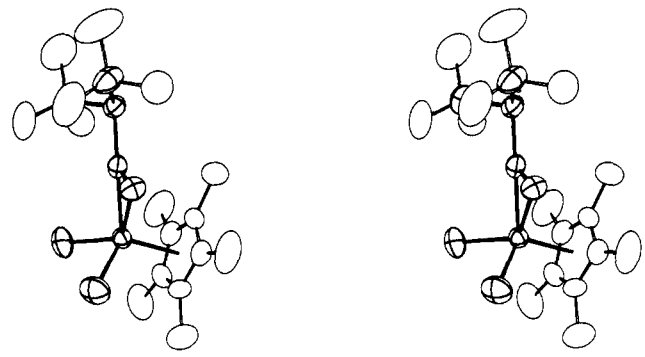

Figure 3. Stereoview of $Cp^*HfCl_2\{\eta^2\text{-}C(O)P(CMe_3)_2\}$ (**12**).

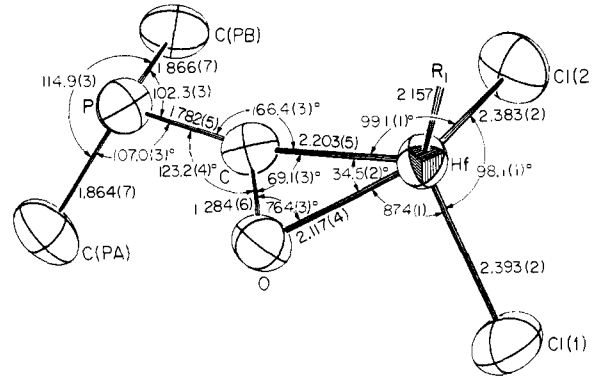


Figure 4. Skeletal view of $Cp^*HfCl_2\{\eta^2\text{-}C(O)P(CMe_3)_2\}$ (**12**), with selected bond distances (Å) and angles (deg).

multiple bonding between the C(acyl) and adjacent carbon atom is observed. The $^{13}C\{^1H\}$ spectrum of the labeled complex, $Cp^*HfCl_2\{\eta^2\text{-}^{13}C(O)P(CMe_3)_2\}$, displays a doublet at 3.03 ppm ($^1J_{PC}$ = 101 Hz), attributable to the carbonyl carbon atom. This observed shift is at very much higher field than characteristic low-field, "carbene-like" or "carbenium-like" acyl and carboxyamide values (Table II) and suggests significant $\pi$-bonding between carbonyl carbon and phosphorus atoms. Together, these data clearly indicate a substantial contribution of canonical form C to the overall valence bonding description.

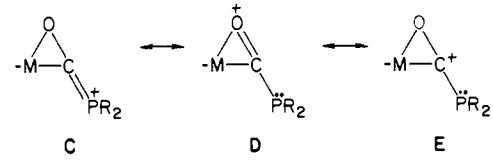


The room temperature 90-MHz $^1H$ NMR spectrum of **12** exhibits a single *tert*-butylmethyl resonance at 1.31 ppm for the inequivalent (vide infra) phosphide *tert*-butyl groups, and hence rotation about the C(acyl)–P bond is rapid on the NMR time scale. Upon cooling, the *tert*-butyl doublet broadens and coalesces at −58 °C. The slow exchange limit for **12** was not resolved at 90 MHz; however, the 500-MHz $^1H$ NMR spectrum for **12** at −93 °C displays a pair of doublets ($^3J_{PH}$ = 10.7, 12.3 Hz) for the inequivalent *tert*-butyl groups with $\Delta\nu$ = 143 ± 2 Hz, corresponding to a frequency separation of 25.7 ± 0.4 Hz at 90-MHz observation frequency. From these values, $\Delta G^\ddagger$ (−58 °C) for rotation about the C–P bond is calculated[36] to be 10.7 ± 0.1 kcal $mol^{-1}$. This observed rotational barrier is somewhat lower than barriers found for transition-metal $\eta^1$-carboxyamides (14–24 kcal $mol^{-1}$)[33] and is far lower than the rotational barrier estimated for $Cp^*_2ThCl(\eta^2\text{-}C(O)(NMe_2)$ (>23 kcal $mol^{-1}$).[33] These values reflect the extent of multiple C–E (E=N, P) bonding and are consistent with trends observed for organic amides and acylphosphines.[37]

(28) Although no adduct of **1** with $PMe_3$ was observed down to −70 °C, variable temperature $^1H$ NMR revealed a steady downfield shift ($\Delta\delta$ = 0.3 ppm at −70 °C) for the *tert*-butyl resonances, suggestive of an equilibrium involving a metal–phosphine interaction. No such shift was observed was **1** in the absence of $PMe_3$.

(29) Fagan, P. J.; Manriquez, J. M.; Marks, T. J.; Day, V. W.; Vollmer, S. H.; Day, C. S. *J. Am. Chem. Soc.* **1980**, *102*, 5393.

(30) Fachinetti, G.; Floriani, C.; Marchetti, F.; Merlino, S. *J. Chem. Soc., Chem. Commun.* **1976**, 522.

(31) Erker, G.; Rosenfeldt, F. *Angew. Chem., Int. Ed. Engl.* **1978**, *17*, 605.

(32) Lappert, M. F.; Luong-Thi, N. T.; Milne, C. R. C. *J. Organomet. Chem.* **1979**, *174*, C35.

(33) Fagan, P. J.; Manriquez, J. M.; Vollmer, S. H.; Day, C, S.; Day, V. W.; Marks, T. J. *J. Am. Chem. Soc.* **1981**, *103*, 2206.

(34) Cramer, R. E.; Maynard, R. B.; Paw, J. C.; Gilje, J. W. *Organometallics* **1982**, *1*, 869.

(35) Moore, E. J. Ph.D. Thesis, California Institute of Technology, 1984.

(36) Using the Eyring equation, with $k_c$(exchange) rate at coalescence temperature ($s^{-1}$) calculated from the Gutowsky-Holm relation: $k_c = (\pi/2^{1/2})\Delta\nu$; Gutowsky, H. S.; Holm, C. H. *J. Chem. Phys.* **1956**, *25*, 1228.

**7. Crystal Structure of $Cp^*HfCl_2\{\eta^2\text{-}C(O)P(CMe_3)_2\}$ (12).** Complex **12** represents the first example of a metal-ligated carboxyphosphide moiety. In order to substantiate the unusual coordination and ligand geometries suggested by the preceding spectroscopic data, the structure of **12** has been determined by X-ray diffraction methods. The molecular structure of $Cp^*HfCl_2\{\eta^2\text{-}C(O)P(CMe_3)_2\}$ is presented as a stereoview in Figure 3, and a skeletal view of the immediate ligation about the hafnium and phosphorus atoms with relevant bond distances and angles is given in Figure 4.

The hafnium coordination geometry may be described as a distorted tetrahedron, if $\eta^5\text{-}C_5(CH_3)_5$ and $\eta^2\text{-}C(O)P(CMe_3)_2$ ligands are considered to each occupy a single site. The four-ring centroid–Hf–X (X = Cl and Y, where Y is defined as the midpoint of the C–O vector) angles vary from 109.7 (1)° to 116.1 (1)°, and the remaining three angles are Cl(1)–Hf–Cl(2) = 98.0 (1)°, Cl(1)–Hf–Y = 101.1°, and Cl(2)–Hf–Y = 112.9°. The Hf–Cl bond lengths of 2.393 (2) and 2.383 (2) Å are somewhat shorter than Hf–Cl values reported for $(CH_2)_3(C_5H_4)_2HfCl_2$ (2.417 (3), 2.429 (2) Å)[38] and $[(SiMe_3)_2N]_3HfCl$ (2.436 (5) Å).[39] Furthermore, Hf–C(ring) values (2.459 (6)–2.471 (6) Å) are significantly contracted relative to average values for $Cp^*_2Hf(H)(\eta^3\text{-}CH_2CHCH_2)$ (2.54 and 2.55 Å)[15] and $[Cp^*HfMe(\mu\text{-}H)\{\eta\text{-}P(CMe_3)_2\}]_2$ (2.57 Å) and for $(\eta^5\text{-}C_5H_5)$ complexes $[Cp_2HfMe_2$ (2.50 (1) Å)[18] and $[Cp_2HfMe]_2O$ (2.513 (5) Å)].[17] These observations are consistent with the known dependence of bond lengths on coordination number. Defining the effective coordination number of cyclopentadienyl ligands as three, the coordination numbers of $[(CH_2)_3(C_5H_4)_2]HfCl_2$ and **12** are eight and seven, respectively. Since the effective ionic radius of Hf(IV) (eight coordination) is 0.83 Å and that of Hf(IV) (seven coordination) is 0.76 Å,[40] an approximately 0.07-Å difference in Hf–Cl and Hf–C(ring) bond lengths is anticipated, in reasonable agreement with the observed values.

The coordination geometry of the carboxyphosphide ligand in **12** is similar to that reported for other dihaptoacyl and $\eta^2$-carboxyamide structures. The C–O bond distance for **12**, 1.284 (6) Å, is somewhat longer than values reported for simple $\eta^2$-acyl complexes $Cp_2ZrMe(\eta^2\text{-}C(O)Me)$ (1.211 (8) Å)[30] and $Cp_2ThCl(\eta^2\text{-}C(O)CH_2CMe_3)$ (1.18 (3) Å)[29] and is similar to C–O bond distances reported for $c\text{-}Cp^*_2ZrH(\eta^2\text{-}C(O)CHPMe_3)$ (1.303 (3) Å)[35] and $Cp^*_2U(\eta^2\text{-}C(O)NMe_2)_2$[33] (1.275 Å av). The Hf–O distance, 2.117 (4) Å, is comparable to reported Hf–O values, 1.94–2.25 Å,[17,41] and is 0.08 Å shorter than the Hf–C(acyl) bond, reflecting the high oxophilicity of Hf(IV).

Comparison of the carboxyphosphide moiety in **12** with reported acylphosphine structures is also revealing. Whereas C(acyl)–P bond distances in $Fe_2(CO)_5\{Ph_2PC(O)C(R)CC(R')C(R'')\}$ (1.918 (6) Å),[42] $(CMe_3)_2PC(O)C(O)P(CMe_3)_2$ (1.88 Å),[43] and $CH_3C(O)P(CH_3)_2$ (1.87 (3) Å)[44] are essentially identical with the remaining C(alkyl)–P bond lengths, the C(acyl)–P bond in **12**, 1.782 (5) Å, is 0.09 Å shorter, implying significant P=C double bond character. This observation is in accord with the 10.7-kcal rotational barrier about the P–C(acyl) bond and is consistent with a contribution of hybrid structure C to the composite valence-bonding description of **12**. Overall, the $\eta^2$-carboxyphosphide ligand is planar to within 0.06 Å and may best be described as a valence-delocalized three-electron ligand. The geometry about the phosphorus atom is pyramidal (vis-ā-vis the planar nitrogen for $M(\eta^2\text{-}CONR_2)$ complexes[33]), the sum of C–P–C(PA) + C–P–C(PB) + C(PA)–P–C(PB) angles totaling 324.2 (3)°. Thus canonical forms **D** and **E** are also important contributors to the description of the bonding $Hf\{\eta^2\text{-}C(O)P(CMe_3)_2\}$.

## Conclusions

Although the initial goal of preparing reactive hydridophosphide complexes of hafnium was not realized, the results described herein are enlightening, nonetheless. Unlike the related dialkylamide and alkoxide complexes $Cp^*HfMe_2X$ (X = $NCHMe_2$, $NMe_2$, $OCMe_3$, and $OCHMe_2$),[45] which react with $H_2$ only at elevated temperatures to form methane and other uncharacterized products, alkyl derivatives with phosphido ancillary ligand react with $H_2$ at room temperature to give alkane and well-defined hydride products in several cases. The origin of the enhanced reactivity of the Hf–alkyl bonds toward $H_2$ is uncertain. One possible explanation is that the weaker interaction of the phosphide lone pair with the hafnium metal center (relative to the strong $\pi$-donors amide and alkoxide) affords a level of valence unsaturation more conductive to a four-center interaction. Alternatively, the greater polarizability of soft phosphide ligand compared to hard, first-row heteroatom ligands may better stabilize a four-center hydrogenolysis transition state with dipolar character:

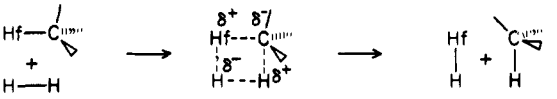

The susceptibility of Hf–P bonds to hydrogenolysis and CO insertion is attributed to the rather low value of the $Hf{=}PR_2$ bond energy, anticipated to be substantially less than the 88 kcal/mol$^{-1}$ value reported for $\bar{D}(Hf{=}NEt_2)$.[26] Accordingly, analogous hydrogenolysis and CO insertion for the related amides $Cp^*HfCl_2NR_2$ (R = $CHMe_2$, Me, and $SiMe_3$) are not observed.[45] Our findings have some bearing on the proposed use of $PR_2$ as a stabilizing ligand in bimetallic and cluster chemistry, particularly for early transition-metal systems, and reinforce the conclusions of others[5] that dialkylphosphide ligands may not always function as innocent bridging ligands.

## Experimental Section

**General Considerations.** All manipulations were performed by using either glovebox or high vacuum line techniques. Solvents were purified by vacuum transfer first from $LiAlH_4$ or benzophenone ketyl and then from "titanocene".[46] $LiP(CMe_3)_2$ was prepared by literature methods.[47] Trimethylphosphine (Strem) was stored under vacuum and distilled prior to use. Hydrogen and deuterium (Matheson) were purified by passage over MnO on Vermiculite[48] and activated 4-Å molecular sieves. Ethylene, carbon monoxide, and $^{13}C$ carbon monoxide (Monsanto-Mound) were used as received. Elemental analyses were determined by Alfred Bernhardt, Dornis and Kolbe, Galbraith, and C.I.T. Analytical Laboratories.

$^1H$ NMR spectra were recorded in $C_6D_6$ by using Varian EM-390, Jeol FX900, and Bruker 500-MHz spectrometers. $^{13}C$ and $^{31}P$ NMR spectra were obtained by using a Jeol FX900 spectrometer. Infrared spectra were measured on a Beckman 4240 spectrometer as Nujol mulls and are reported in inverse centimeters.

Several reactions were conducted in sealed NMR tubes and monitored by $^1H$ NMR spectroscopy. A typical example is the reaction of $Cp^*HfCl(CH_2Ph)\{P(CMe_3)_2\}$ (**4**) with $H_2$; **4** (20 mg, 0.04 mmol) was transferred to an NMR tube sealed to a ground-glass joint and fitted with

(37) Values reported for hindered rotation in organic amides range from 15 to 30 kcal (ref 44a). Although direct measurement of acylphosphine rotational barriers has not been reported, calculations suggest an upper limit of ~6 kcal (ref 44bc). (a) Kessler, H. *Angew. Chem., Int. Ed. Engl.* **1970**, *9*, 219. (b) Egan, W.; Mislow, K. *J. Am. Chem. Soc.* **1971**, *93*, 1805. Kostyanovskii, R. G.; Elnatanov, Y. I.; Zakharov, K. S.; Zagurskaya, L. M. *Dokl. Akad. Nauk. SSSR* **1974**, *219*, 1021. (c) Dougherty, D. A.; Mislow, K.; Whangbo, M.-H. *Tetrahedron Lett.* **1979**, 2321.

(38) Saldarriaga-Molina, C. H.; Clearfield, A.; Bernal, I. *Inorg. Chem.* **1974**, *13*, 2880.

(39) Raymond, K. N.; Eigenbrot, C. W., Jr. *Acc. Chem. Res.* **1980**, *13*, 276.

(40) Shannon, R. D. *Acta Crystallogr., Sect. A* **1976**, *32A*, 751.

(41) (a) Tranqui, D.; Laugier, J.; Boyer, P.; Vulliet, P. *Acta Crystallogr., Sect. B* **1978**, *34B*, 767. Tranqui, D.; Tissier, A.; Laugier, J.; Boyer, P. *Ibid.* **1977**, *33b*, 392. (b) Stutte, B.; Batzel, V.; Boese, R.; Schmid, G. *Chem. Ber.* **1978**, *111*, 1603.

(42) Smith, W. F.; Taylor, N. J.; Carty, A. J. *J. Chem. Soc., Chem. Commun.* **1976**, 896.

(43) Becker, H.-J.; Fenske, D.; Langer, E.; Prokscha, H. *Monatsh. Chem.* **1980**, *111*, 749.

(44) Khaikin, L. S.; Adrutskaya, L. G.; Grikina, O. E.; Vilkov, L. V.; El'Natov, Y. I.; Kostyanovskii, R. G. *J. Mol. Struct.* **1977**, *37*, 237.

(45) Roddick, D. M., unpublished results.

(46) Marvich, R. H.; Brintzinger, H. H. *J. Am. Chem. Soc.* **1971**, *94*, 2046.

(47) Hoffmann, H.; Schellenbeck, P. *Chem. Ber.* **1966**, *99*, 1134.

(48) Brown, T. L.; Dickerhoof, D. W.; Bafus, D. A.; Morgan, G. L. *Rev. Sci. Instrum.* **1962**, *33*, 491.

a Teflon needle valve adapter. Benzene-$d_6$ (0.3 mL) was distilled into the tube at 77 K, 730 torr of $H_2$ was admitted, and the tube was sealed with a torch.

**Procedures.** **Cp*HfCl$_2${P(CMe$_3$)$_2$} (1).** Cp*HfCl$_3$[49] (4.04 g, 9.6 mmol) and LiP(CMe$_3$)$_2$ (1.48 g, 9.7 mmol) were placed in a flask, and ca. 40 mL of diethyl ether was distilled in at −78 °C. Initially pale yellow, the reaction mixture turned deep green upon warming to room temperature. After stirring at 25 °C for 12 h, the diethyl ether was replaced with 30 mL of petroleum ether, the solution was filtered, and the precipitate was washed with petroleum ether. Concentration and crystallization at −78 °C followed by sublimation (90 °C, $10^{-4}$ torr) yielded 2.84 g of deep-green **1** (56%): IR 1360, 1163 (s), 1020, 798 cm$^{-1}$. Anal. Calcd. for $C_{18}H_{33}Cl_2HfP$: C, 40.81; H, 6.28; P, 5.85; Cl, 13.40. Found: C, 40.38; H, 7.10; P, 5.65; Cl, 13.38. Solution molecular weight ($C_6D_6$) calcd 529, found 512.[50]

**Cp*HfCl{P(CMe$_3$)$_2$}$_2$ (2).** Cp*HfCl$_3$ (0.50 g, 1.19 mmol) and LiP(Cme$_3$)$_2$ (0.452 g, 2.97 mmol) were placed in a flask, and 20 mL of diethyl ether was distilled in at −78 °C. The reaction mixture was warmed to room temperature and stirred for 12 h. The volatiles were removed in vacuo and petroleum ether was distilled in. The solution was filtered and concentrated to ca. 7 mL; cooling to −78 °C afforded 0.485 g (64%) of dark olive green **2**: IR 1361, 1166 (s), 1023, 813 cm$^{-1}$. Anal. Calcd for $C_{56}H_{51}ClHfP_2$: C, 48.83; H, 8.04; Cl, 5.54; P, 9.68. Found: C, 48.76; H, 7.93; Cl, 5.48; P, 9.64.

**Cp*HfCl(CH$_2$CMe$_3$){P(CMe$_3$)$_2$} (3).** Thirty milliliters of diethyl ether was distilled onto a mixture of Cp*HfCl$_2${P(CMe$_3$)$_2$} (0.500 g, 0.95 mmol) and LiCH$_2$CMe$_3$ (0.77 g, 0.99 mmol) at −78 °C, and the reaction mixture was warmed slowly to room temperature with stirring. After 12 h, the diethyl ether was removed and petroleum ether was distilled in. Filtrating, washing, and crystallizing at −78 °C yielded only 0.109 g (19%) of a highly soluble maroon solid, >90% **3**, by $^1$H NMR: IR 1360, 227 (sh), 1215, 1156, 1022 cm$^{-1}$.

**Cp*HfCl(CH$_2$Ph){P(CMe$_3$)$_2$} (4).** The procedure for **3** was followed except 0.67 g (1.27 mmol) of **1** and 0.17 g (1.31 mmol) of KCH$_2$Ph were combined in 25 mL of diethyl ether. Removal of solvent and recrystallization from petroleum ether of the blue-green reaction product afforded 0.54 g (73%) of violet, crystalline **4**: IR 1595, 1583 (sh), 1484, 1360, 1197, 1162, 1045, 1023, 996, 812 (sh), 796, 743 (sh), 694 cm$^{-1}$; UV $\lambda_{max}$ 580 nm. Anal. Calcd for $C_{25}H_{40}ClHfP$: C, 51.28; H, 6.89; Cl, 6.05; P, 5.29. Found: C, 51.21; H, 6.96; Cl, 5.96; P, 5.40.

**Cp*HfMeCl$_2$.** Cp*HfCl$_3$ (3.705 g, 8.82 mmol) was placed in a flask, and ca. 100 mL of diethyl ether was distilled in at −78 °C. MeMgBr (8.84 mmol) (3.05 mL, 2.9 M) was syringed into the ether solution at −78 °C under argon counterflow, and the reaction mixture was warmed to room temperature. Removal of solvent and recrystallization from petroleum ether after 2 h[51] afforded 3.05 g (87%) of white crystalline Cp*HfMeCl$_2$: IR 1486, 1424, 1150 (st), 1024 (st), 799, 540, 460 cm$^{-1}$. Anal. Calcd for $C_{11}H_{18}Cl_2Hf$: C, 33.06; H, 4.54. Found: C, 32.98; H, 4.44.

**Cp*HfMe$_2$Cl.** The procedure for Cp*HfMeCl$_2$ was followed except 6.54 g (15.6 mmol) of Cp*HfCl$_3$ and 11 mL of 2.9 M MeMgBr (31.9 mmol) were combined in 100 mL of ether. Removal of solvent and recrystallization from petroleum ether after 1 day[51] yielded 5.17 g (88%) of off-white Cp*HfMe$_2$Cl: IR 1485, 1138, 1023, 802 cm$^{-1}$. Anal. Calcd for $C_{12}H_{21}ClHf$: C, 38.00; H, 5.58; Hf, 47.07. Found: C, 37.97; H, 5.66; Hf, 46.99.

**Cp*HfPhCl$_2$.** The procedure for Cp*HfMeCl$_2$ was followed except 1.11 g (2.64 mmol) of Cp*HfCl$_3$ and 1.2 mL of 2.2 M PhLi (2.64 mmol) were combined in 50 mL of ether. Removal of solvent and recrystallization from petroleum ether gave 0.895 g (73%) of Cp*HfPhCl$_2$: IR 3050, 1592, 1490 (sh), 1480 (sh), 1412, 1282, 1064, 1028, 991, 890, 730, 703 cm$^{-1}$. Anal. Calcd for $C_{16}H_{20}Cl_2Hf$: C, 41.62; H, 4.37. Found: C, 42.03; H, 4.47.

**Cp*HfMe$_2${P(CMe$_3$)$_2$} (5).** Cp*HfMe$_2$Cl (2.35 g, 6.20 mmol) and LiP(CMe$_3$)$_2$ (1.03 g, 6.77 mmol) were placed in a flask and 60 mL of diethyl ether was distilled in. Initially light yellow, the reaction mixture quickly turned purple and then deep red upon warming to room temperature. After 12 h, the diethyl ether was replaced with petroleum ether, the solution was filtered, and the precipitate was washed thoroughly. Concentration and crystallization at −78 °C followed by sublimation (90 °C, $10^{-4}$ torr) yielded 1.76 g of magenta **5** (58%): IR 1358, 1166, 1134, 1018 cm$^{-1}$. Anal. Calcd for $C_{20}H_{39}PHf$: C, 49.13; H, 8.04; P, 6.33. Found: C, 48.85; H, 8.45; P, 6.42.

**Cp*HfCl(Ph){P(CMe$_3$)$_2$} (6).** The procedure for **5** was followed except 0.495 g (1.07 mmol) of Cp*Hf(Ph)Cl$_2$ and 0.165 g (1.08 mmol) of LiP(CMe$_3$)$_2$ were combined in 30 mL of diethyl ether. Removal of solvent and recrystallization from petroleum ether afforded 0.275 g (44%) of red–purple Cp*HfCl(Ph){P(CMe$_3$)$_2$}: IR 3050, 1361, 1165, 1022, 990, 720, 700 cm$^{-1}$. Anal. Calcd for $C_{24}H_{3}ClPHf$: C, 50.44; H, 6.70. Found: C, 49.35; H, 6.71.

**[Cp*HfMe(μ-H){μ-P(CMe$_3$)$_2$}]$_2$ (7).** A thick-walled glass reaction vessel with a Teflon needle valve charged with 0.35 g (0.72 mmol) of **5**, 10 mL of toluene and ca. 3 atm of $H_2$ was stirred at room temperature for 1 week. The precipitate was thoroughly washed with petroleum ether and dried in vacuo, yielding 0.21 g (62%) of light-yellow **7**: IR 1510, 1485 (sh), 1352, 1161, 1132, 1077, 1013, 760 cm$^{-1}$. Anal. Calcd for $C_{38}H_{74}Hf_2P_2$: C, 48.05; H, 7.85; Hf, 37.58. Found: C, 48.13; H, 7.86; Hf, 37.54.

**Reaction of 7 with HCl.** To **7** (0.040 g, 0.042 mmol) was condensed 5 mL of toluene and HCl (ca. 6 equiv). Upon warming to room temperature, a vigorous evolution of gas was observed. One component was identified as $CH_4$ by an independent experiment conducted in an NMR tube. The product $H_2/CH_4$ mixture was passed through a series of liquid $N_2$-cooled traps and collected via a Toepler pump. $H_2 + CH_4$ amounted to 0.14 mmol or 1.7 mmol of $(H_2 + CH_4)$/mmol of Hf. This mixture was removed in a liquid $N_2$ trap. The remaining $CH_4$ collected amounted to 0.070 mmol (0.85 mmol/mmol of Hf), or one-half of the total gas collected (i.e., $H_2/CH_4$ = 1:1). The residue obtained after removal of volatiles was not identified.

**Structure Determination for [Cp*HfMe(μ-H){μ-P(CMe$_3$)$_2$}]$_2$ (7).** Sufficiently large, well-formed orange crystals of **7** were obtained from the slow reaction of **5** and $H_2$ in toluene at 0 °C. A single crystal (0.67 × 0.33 × 0.17 mm) was mounted approximately along the $b$ axis in a glass capillary under $N_2$. A series of oscillation and Weissenberg photographs indicated monoclinic symmetry; the space group $P2_1/c$ was inferred from systematic absences in the photographs and diffractometer data ($0k0$ absent for $k$ odd; $h0l$ absent for $l$ odd). Data were collected on a locally modified Syntex $P2_1$ diffractometer with graphite monochromator. The unit cell parameters (Table III) were obtained by least-squares refinement of 15 $2\theta$ values ($46 < 2\theta < 59°$), where each $2\theta$ value was an average of two measurements, at $\pm 2\theta$. Intensity data was corrected for a 2.3% linear decay, as indicated by the three check reflections, and the data were reduced to $F_o^2$; the form factors for all atoms were taken from ref 52, and those for Hf and P were corrected for anomalous dispersion. The details on data collection are given in Table III.

The position of the Hf atom was derived from the Patterson map, and a series of Fourier maps phased on Hf revealed the remaining non-hydrogen atoms of the complex. Least-squares refinement of atom coor-

**Table III.** Crystal and Intensity Collection Data for [Cp*HfMe(μ-H){μ-P(CMe$_3$)$_2$}]$_2$ (7)

| | |
|---|---|
| formula | $C_{38}H_{74}Hf_2P_2$ |
| fw, g/mol | 767.02 |
| space group | $P2_1/c$ |
| $a$, Å | 11.4848 (21) |
| $b$, Å | 16.447 (5) |
| $c$, Å | 11.8255 (22) |
| $\beta$, deg | 118.915 (11) |
| $V$, Å$^3$ | 1955.1 |
| $Z$ | 4 |
| $D_{calcd}$, g/cm$^3$ | 1.61 g/cm$^3$ |
| crystal size | 0.67 × 0.33 × 0.17 mm |
| λ, Å | 0.7107 (Mo Kα) |
| $\mu$, mm$^{-1}$ | 5.36 mm$^{-1}$ |
| scan range | 1.0° below Kα$_1$, 1.1° above Kα$_2$ |
| refln settings | $+h,+k,\pm l$ |
| $2\theta$ range, scan rate | $3.5 < 2\theta < 36°$, 4.88°/min, 1.0, 3143 |
| backgrd time/scan time, no. of reflns | $35 < 2\theta < 50°$, 2.02°/min, 0.5, 6323 |
| tot no. of av data | 5678 |
| refinement on | $F_o^2$ |
| final no. of parameters | 195 |
| final cycle | total data set; robust refinement |
| $R$ | 0.071 (5503); 0.066 (5413) |
| $R'$ | 0.064 (4693); 0.059 (4603) |
| $S$ | 4.02 (5678); 3.55 (5588) |

[a] Typical $R$ value, number of reflections used in sums given in parentheses. $R'$ refers to $R$ value calculated for reflections with $F_o^2 > 3\sigma_{F^2}$. $S$ is the goodness-of-fit; summations include all reflections. Robust refinement deleted reflections with $|\Delta F|/\sigma_{F^2} > 6$.

(49) Roddick, D. M.; Fryzuk, M. D.; Seidler, P. F.; Hillhouse, G. L.; Bercaw, J. E. *Organometallics* **1985**, *4*, 97.

(50) Molecular weight determined by isothermal distillation using the Singer method. (a) Singer, R. *Justus Liebigs Ann. Chem.* **1930**, *478*, 246. (b) Clark, E. P. *Ind. Eng. Chem., Anal. Ed.* **1941**, *13*, 820.

(51) Prolonged metathesis resulted in significant Cl ⇌ Br exchange, as judged by elemental analysis.

**Table IV.** Atom Coordinates ($\times 10^4$) and $U_{eq}$'s (Å$^2$, $\times 10^4$)

| | $x$ | $y$ | $z$ | $U_{eq}$ |
|---|---|---|---|---|
| Hf | 1291.8 (3) | 544.4 (2) | 276.8 (3) | 224 |
| P | −1183 (2) | 605 (1) | −1978 (2) | 255 |
| C(M) | 1172 (8) | 1709 (5) | 1226 (8) | 384 |
| C(1) | 3720 (7) | 204 (5) | 983 (8) | 338 |
| C(2) | 3700 (8) | 1061 (5) | 1221 (8) | 378 |
| C(3) | 3003 (8) | 1452 (5) | 39 (9) | 364 |
| C(4) | 2545 (8) | 873 (5) | −968 (8) | 328 |
| C(5) | 3013 (8) | 94 (5) | −354 (8) | 330 |
| C(1M) | 4633 (9) | −393 (7) | 1982 (11) | 520 |
| C(2M) | 4530 (10) | 1477 (8) | 2506 (10) | 578 |
| C(3M) | 2917 (11) | 2368 (6) | −155 (10) | 514 |
| C(4M) | 2008 (9) | 1086 (6) | −2361 (9) | 440 |
| C(5M) | 2991 (10) | −685 (6) | −1047 (10) | 458 |
| C(PA) | −1564 (9) | 140 (6) | −3621 (7) | 391 |
| C(PA1) | −2973 (11) | −236 (7) | −4242 (9) | 547 |
| C(PA2) | −562 (11) | −526 (6) | −3367 (9) | 501 |
| C(PA3) | −1490 (11) | 727 (7) | −4599 (9) | 536 |
| C(PB) | −1964 (8) | 1679 (5) | −2294 (8) | 381 |
| C(PB1) | −1015 (10) | 2272 (6) | −2439 (11) | 538 |
| C(PB2) | −2082 (11) | 1929 (6) | −1119 (11) | 506 |
| C(PB3) | −3350 (10) | 1766 (7) | −3477 (10) | 522 |
| H | 424 (118) | −751 (73) | −463 (117) | |

**Table V.** (a) Bond Lengths (Å) and (b) Bond Angles (deg) for $[Cp^*HfMe(\mu\text{-}H)\{\mu\text{-}P(CMe_3)_2\}]_2$ (**7**)

a

| | | | |
|---|---|---|---|
| Hf–Hf′ | 3.250 | C(3)–C(4) | 1.413 (13) |
| Hf–R$_1$[a] | 2.264 | C(4)–C(5) | 1.442 (12) |
| Hf–C(M) | 2.258 (9) | C(1)–C(1M) | 1.504 (14) |
| Hf–H′ | 2.33 (13) | C(2)–C(2M) | 1.512 (15) |
| Hf–H | 2.12 (13) | C(3)–C(3M) | 1.520 (14) |
| Hf–P | 2.805 (2) | C(4)–C(4M) | 1.495 (13) |
| Hf–P′ | 2.807 (2) | C(5)–C(5M) | 1.514 (14) |
| Hf–C(1) | 2.557 (9) | P–C(PA) | 1.931 (10) |
| Hf–C(2) | 2.575 (9) | P–C(PB) | 1.933 (9) |
| Hf–C(3) | 2.589 (9) | C(PA)–C(PA1) | 1.546 (15) |
| Hf–C(4) | 2.564 (9) | C(PA)–C(PA2) | 1.509 (15) |
| Hf–C(5) | 2.537 (9) | C(PA)–C(PA3) | 1.541 (15) |
| C(1)–C(5) | 1.396 (12) | C(PB)–C(PB1) | 1.534 (15) |
| C(1)–C(2) | 1.439 (13) | C(PB)–C(PB2) | 1.517 (15) |
| C(2)–C(3) | 1.388 (13) | C(PB)–C(PB2) | 1.536 (14) |

b

| | | | |
|---|---|---|---|
| H–Hf–H′ | 86 (5) | C(PA1)–C(PA)–P | 108.2 (7) |
| P–Hf–P′ | 109.2 (1) | C(PA2)–C(PA)–P | 107.9 (7) |
| R$_1$–Hf–C(M)[a] | 101.4 (2) | C(PA3)–C(PA)–P | 116.1 (7) |
| R$_1$–Hf–H′ | 111 (3) | C(PB1)–C(PB)–P | 108.3 (7) |
| R$_1$–Hf–H | 162 (4) | C(PB2)–C(PB)–P | 108.0 (7) |
| R$_1$–Hf–P | 120.5 (1) | C(PB3)–C(PB)–P | 116.2 (7) |
| R$_1$–Hf–P′ | 120.5 (1) | C(2)–C(1)–C(5) | 107.1 (8) |
| C(M)–Hf–H′ | 147 (3) | C(3)–C(2)–C(1) | 108.2 (8) |
| C(M)–Hf–H | 62 (4) | C(4)–C(3)–C(2) | 109.5 (8) |
| C(M)–Hf–P | 99.5 (2) | C(5)–C(4)–C(3) | 106.2 (8) |
| C(M)–Hf–P′ | 100.4 (2) | C(1)–C(5)–C(4) | 109.0 (8) |
| H–Hf–P | 68 (3) | C(1M)–C(1)–C(5) | 127.4 (8) |
| H′–Hf–P′ | 62 (4) | C(1M)–C(1)–C(2) | 123.8 (8) |
| H–Hf–P′ | 71 (4) | C(2M)–C(2)–C(1) | 125.3 (9) |
| Hf–H–Hf′ | 94 (5) | C(2M)–C(2)–C(3) | 125.4 (9) |
| Hf–P–Hf′ | 70.8 (1) | C(3M)–C(3)–C(2) | 125.1 (9) |
| C(PA)–P–C(PB) | 108.0 (4) | C(3M)–C(3)–C(4) | 124.8 (8) |
| C(PA)–P–Hf | 125.1 (3) | C(4M)–C(4)–C(3) | 123.9 (8) |
| C(PA)–P–Hf′ | 112.8 (3) | C(4M)–C(4)–C(5) | 128.2 (8) |
| C(PB)–P–Hf | 112.2 (3) | C(5M)–C(5)–C(4) | 125.1 (8) |
| C(PB)–P–Hf′ | 125.2 (3) | C(5M)–C(5)–C(1) | 124.8 (8) |
| C(PA1)–C(PA)–C(PA2) | 109.1 (8) | C(PB1)–C(PB)–C(PB2) | 108.2 (8) |
| C(PA1)–C(PA)–C(PA3) | 108.6 (8) | C(PB1)–C(PB)–C(PB3) | 108.6 (8) |
| C(PA2)–C(PA)–C(PA3) | 106.8 (8) | C(PB2)–C(PB)–C(PB3) | 107.3 (8) |

[a] R$_1$ ≡ ring centroid of Cp* ring [atoms C(1)–C(5M)].

dinates and $U$'s, minimizing $\sum\omega[F_o^2 - (F_c/k)^2]^2$, gave $R = 0.084$. All ring methyl and phosphide *tert*-butyl methyl H atoms and the hydride atom were located from difference maps; all H atoms except the hydride were introduced into the model with fixed coordinates and isotropic $U$'s.

**Table VI.** Crystal and Intensity Collection Data for $Cp^*HfCl_2\{\eta^2\text{-}C(O)P(CMe_3)_2\}$ (**12**)

| | |
|---|---|
| formula | $C_{19}H_{33}Cl_2HfOP$ |
| fw, g/mol | 557.83 |
| space group | $P2_12_12_1$ |
| $a$, Å | 14.9191 (15) |
| $b$, Å | 9.9521 (10) |
| $c$, Å | 15.7794 (18) |
| $V$, Å$^3$ | 2342.8 |
| $Z$ | 4 |
| $D_{calcd}$, g/cm$^3$ | 1.64 |
| crystal size | 0.33 × 0.75 × 0.33 ([100] × [010] × [001]) |
| λ, Å | 0.7107 (Mo Kα) |
| $\mu$, mm$^{-1}$ | 4.85 |
| scan range | 1.2° below Kα$_1$, 1.2° above Kα$_2$ |
| 2θ limits, scan rate, backgrd time/scan time, no. of reflns | 4–35°, 2.02°/min, 1107 ($+h,+k,\pm l$)<br>17–35°, 3.91°/min, 738 ($+h,+k,\pm l$)<br>34–46°, 2.93°/min, 2746 ($+h,+k,\pm l$)<br>4–36°, 4.88°/min, 1881 ($+h,-k,\pm l$)<br>45–50°, 2.02°/min, 1160 ($+h,+k,\pm l$)<br>45–56°, 2.02°/min, 1760 ($+h,+k,\pm l$) |
| tot no. of av data | 5760 |
| refinement on | $F_o^2$ |
| final no. of parameters | 218 |
| final agreement $R$ ($F_o^2 > 0$) | 0.040 (5570)[a] |
| $R'$ | 0.030 (4609) |
| $S$ | 1.66 (5760) |

[a] Typical $R$ value, number of reflections used in sums given in parentheses. $R'$ refers to $R$ value calculated for reflections with $F_o^2 > 3\sigma_{F^2}$. $S$ is the goodness-of-fit.

**Table VII.** Atom Coordinates ($\times 10^4$) and $U_{eq}$'s (Å$^2$, $\times 10^4$)

| | $x$ | $y$ | $z$ | $U_{eq}$ |
|---|---|---|---|---|
| Hf | 7663.7 (1) | 6103.5 (2) | 7536.5 (1) | 403 |
| P | 7541 (1) | 8745 (1) | 9407.3 (8) | 456 |
| Cl(1) | 8587 (1) | 6558 (2) | 6330.2 (9) | 718 |
| Cl(2) | 6255 (1) | 6681 (2) | 6925 (1) | 724 |
| C | 7730 (4) | 7661 (5) | 8526 (3) | 425 |
| O | 8515 (3) | 7397 (4) | 8235 (2) | 498 |
| C(1) | 7026 (4) | 4233 (6) | 8368 (4) | 554 |
| C(2) | 7863 (5) | 4539 (5) | 8736 (3) | 516 |
| C(3) | 8527 (4) | 4242 (6) | 8151 (4) | 549 |
| C(4) | 8112 (5) | 3731 (5) | 7418 (4) | 551 |
| C(5) | 7182 (4) | 3729 (5) | 7554 (4) | 562 |
| C(1M) | 6118 (6) | 4359 (8) | 8799 (6) | 1133 |
| C(2M) | 8030 (7) | 4989 (6) | 9649 (4) | 929 |
| C(3M) | 9522 (5) | 4390 (8) | 8276 (6) | 1024 |
| C(4M) | 8583 (7) | 3146 (8) | 6653 (5) | 1016 |
| C(5M) | 6494 (7) | 3213 (8) | 6945 (5) | 1112 |
| C(PA) | 8485 (4) | 9972 (6) | 9430 (5) | 627 |
| C(PA1) | 9318 (5) | 9153 (8) | 9699 (5) | 819 |
| C(PA2) | 8685 (6) | 10627 (7) | 8572 (6) | 1019 |
| C(PA3) | 8312 (6) | 11038 (10) | 10085 (7) | 1442 |
| C(PB) | 6423 (4) | 9483 (6) | 9153 (4) | 600 |
| C(PB1) | 6168 (6) | 10486 (10) | 9821 (6) | 1170 |
| C(PB2) | 5765 (5) | 8311 (8) | 9175 (5) | 808 |
| C(PB3) | 6371 (5) | 10165 (8) | 8296 (5) | 923 |

The refinement of non-hydrogen atoms in the Hf complex with anisotropic $U_{ij}$'s and the coordinates of the hydride atom with fixed isotropic $U$ using all the data (5678 reflections) led to $R = 0.071$; the isotopic secondary extinction coefficient was refined, giving a value of 0.69 (6) × 10$^{-6}$. Robust refinement, with 90 reflections deleted having values of $|\Delta F|/\sigma_{F^2} > 6$, led to a final $R = 0.066$. The final $\Delta F$ map showed several large features indicative of residual adsorption errors: symmetric pairs of peaks located approximately 0.75 Å from the heavy atoms (~5 e$^-$/Å$^3$ around Hf, ~2 e$^-$/Å$^3$ around P). Final atom coordinates are given in Table IV. Bond lengths and angles are given in Table V. All calculations were carried out on a VAX 11/780 computer by using the CRYRM system of programs.

**$Cp^*HfMe(Et)\{P(CMe_3)_2\}$ (8).** To **7** (0.025 g, 0.027 mmol) and 0.3 mL of benzene-$d_6$ in an NMR tube was condensed $C_2H_4$ (0.16 mmol), and the tube was sealed off. After 1$^1$/$_2$ hours at 80 °C the solution was deep red; $^1$H NMR indicated a single (>90% pure) soluble product, tentatively identified as the ethylene insertion product **8**.

**$[Cp^*Hf(\mu\text{-}H)\{\mu\text{-}P(CMe_3)_2\}]_2$ (9).** A solution of $Cp^*HfCl\{P(CMe_3)_2\}_2$ (**2**) (0.391 g, 0.55 mmol) in 20 mL of toluene was stirred under 1 atm

**Table VIII.** (a) Bond Lengths (Å) and (b) Bond Angles (deg) for $Cp^*HfCl_2\{\eta^2\text{-}C(O)P(CMe_3)_2\}$ (**12**)

a

| | | | |
|---|---|---|---|
| Hf–[a]$R_1$ | 2.157 | C(2)–C(3) | 1.386 (9) |
| Hf–Cl(1) | 2.393 (2) | C(3)–C(4) | 1.407 (9) |
| Hf–Cl(2) | 2.383 (2) | C(4)–C(5) | 1.404 (8) |
| Hf–C | 2.203 (5) | C(1)–C(1M) | 1.521 (11) |
| Hf–O | 2.117 (4) | C(2)C(2M) | 1.528 (9) |
| Hf–C(1) | 2.468 (6) | C(3)–C(3M) | 1.506 (11) |
| Hf–C(2) | 2.469 (6) | C(4)–C(4M) | 1.513 (10) |
| Hf–C(3) | 2.456 (6) | C(5)–C(5M) | 1.497 (11) |
| Hf–C(4) | 2.461 (6) | C(PA)–C(PA1) | 1.546 (10) |
| Hf–C(5) | 2.471 (6) | C(PA)–C(PA2) | 1.533 (11) |
| C–O | 1.284 (6) | C(PA)–C(PA3) | 1.503 (12) |
| P–C | 1.782 (5) | C(PB)–C(PB1) | 1.500 (1) |
| P–C(PA) | 1.864 (7) | C(PB)–C(PB2) | 1.525 (10) |
| P–C(PB) | 1.866 (7) | C(PB)–C(PB3) | 1.516 (10) |
| C(1)–C(5) | 1.398 (8) | | |
| C(1)–C(2) | 1.410 (8) | | |

b

| | | | |
|---|---|---|---|
| [a]$R_1$–Hf–Cl(1) | 116.1 (1) | C(1M)–C(1)–C(5) | 126.1 (6)) |
| $R_1$–Hf–Cl(2) | 114.9 (1) | C(1M)–C(1)–C(2) | 125.9 (6) |
| $R_1$–Hf–C | 112.7 (1) | C(2M)–C(2)–C(1) | 126.6 (5) |
| $R_1$–Hf–O | 109.7 (1) | C(2M)–C(2)–C(3) | 125.0 (6) |
| Cl(1)–Hf–Cl(2) | 98.1 (1) | C(3M)–C(3)–C(2) | 126.7 (6) |
| Cl(1)–Hf–C | 113.9 (1) | C(3M)–C(3)–C(4) | 125.2 (6) |
| Cl(1)–Hf–O | 87.4 (1) | C(4M)–C(4)–C(3) | 126.2 (6) |
| Cl(2)–Hf–C | 99.1 (1) | C(4M)–C(4)–C(5) | 125.4 (6) |
| Cl(2)–Hf–O | 126.4 (1) | C(5M)–C(5)–C(4) | 125.5 (6) |
| C–Hf–O | 34.5 (2) | C(5M)–C(5)–C(1) | 126.8 (6) |
| Hf–C–P | 166.4 (3) | P–C(PA)–C(PA1) | 105.5 (5) |
| Hf–C–O | 69.1 (3) | P–C(PA)–C(PA2) | 114.1 (5) |
| P–C–O | 123.2 (4) | P–C(PA)–C(PA3) | 110.3 (5) |
| Hf–O–C | 76.4 (3) | C(PA1)–C(PA)–C(PA2) | 108.1 (6) |
| C–P–C(PA) | 107.0 (3) | C(PA1)–C(PA)–C(PA3) | 108.8 (6) |
| C–P–C(PB) | 102.3 (3) | C(PA2)–C(PA)–C(PA3) | 109.9 (6) |
| C(PA)–P–C(PB) | 114.9 (3) | P–C(PB)–C(PB1) | 109.8 (5) |
| C(2)–C(1)–C(5) | 108.0 (5) | P–C(PB)–C(PB2) | 105.6 (4) |
| C(3)–C(2)–C(1) | 108.1 (5) | P–C(PB)–C(PB3) | 114.4 (5) |
| C(4)–C(3)–C(2) | 108.1 (5) | C(PB1)–C(PB)–C(PB2) | 109.3 (6) |
| C(5)–C(4)–C(3) | 108.0 (5) | C(PB1)–C(PB)–C(PB3) | 108.4 (6) |
| C(1)–C(5)–C(4) | 107.7 (5) | C(PB2)–C(PB)–C(PB3) | 109.3 (6) |

[a] $R_1$ ≡ ring centroid of Cp* ring [atoms C(1)–Cn(5M)].

of $H_2$ for 3 h. The solution was filtered, and the light-yellow solid was washed thoroughly with toluene and dried in vacuo: yield 87%; IR 1517, 1483 (sh), 1373, 1358, 1162, 1073, 1017, 834, 806, 770 $cm^{-1}$. Anal. Calcd for $C_{36}H_{68}Cl_2Hf_2P$: C, 43.64; H, 6.92. Found: C, 43.90; H, 6.88.

**$Cp^*HfCl(Et)(PMe_3)$ (11).** A thick-walled glass reaction vessel with a Teflon needle valve was charged with 0.527 g (0.996 mmol) of **1**, 10 mL of toluene, 6.67 mmol of $C_2H_4$, 5.00 mmol of $PMe_3$, and ca. 3 atm of $H_2$ (~3.6 mmol) and stirred at room temperature. After 2 days, solvent removal and recrystallization from petroleum ether yielded 0.353 g (72%) of off-white **11**: IR 1487, 1425, 1302, 1283, 1022, 961 (s), 941, 919 (sh), 732 (s) $cm^{-1}$. Anal. Calcd for $C_{15}H_{29}Cl_2HfP$: C, 36.79; H, 5.97. Found: C, 36.54; H, 5.83.

**$Cp^*HfCl_2\{\eta^2\text{-}C(O)P(CMe_3)_2\}$ (12).** A solution of 0.497 g (0.940 mmol) of $Cp^*HfCl_2\{P(CMe_3)_2\}$ (**1**) in 15 mL of petroleum ether was stirred under 900 torr of CO for 20 min. Filtrating, washing with cold petroleum ether, and drying in vacuo yielded 0.380 g (73%) of bright-yellow **12**: IR 1400, 1363 (sh), 1350 (s) ($\nu$(C–O)), 1175, 1029, 937, 854, 811, 720, 620, 520 $cm^{-1}$. Anal. Calcd for $C_{19}H_{33}Cl_2HfOP$: C, 40.91; H, 5.96; Cl, 12.71; P, 5.55. Found: C, 41.00; H, 6.03; Cl, 12.74; P, 5.70.

**Structure Determination for $Cp^*HfCl_2\{\eta^2\text{-}C(O)P(CMe_3)_2\}$ (12).** A single crystal (0.33 × 0.75 × 0.33 mm) grown from a pentane/benzene solution was mounted in a glass capillary under $N_2$. Oscillation and Weissenberg photographs indicated orthorhombic symmetry; the space group $P2_12_12_1$ was inferred from the systematic absences in the photographs and in the diffractometer data ($h00$ absent for $h$ odd; $0k0$ absent for $k$ odd; $00l$ absent for $l$ odd). Data were collected on a locally modified Syntex $P2_1$ diffractometer with graphite monochromator; details on unit cell parameters and the data collection are given in Table VI. Intensity data was corrected for a 1.7% linear decay, as indicated by the three check reflections, and the data were reduced to $F_o^2$.[53]

The position of the Hf atom was derived from the Patterson map, and a series of Fourier maps phased on Hf revealed the remaining non-hydrogen atoms of the complex. Least-squares refinement of atom coordinates and $U$'s, minimizing $\sum\omega[F_o^2 - (F_c/k)^2]^2$, gave $R = 0.053$. All hydrogens were located from difference maps and introduced into the model with fixed coordinates and isotropic $U$'s. The refinement of non-hydrogen atoms in the Hf complex with anisotropic $U_{ij}$'s using all the data (5760 reflections) led to $R = 0.040$ and $S = 1.66$, with refinement of the anisotropic secondary extinction coefficient = 0.58 (3) × $10^{-6}$.

The final $\Delta F$ map showed residual peaks of 1.0 and 1.2 $e^-/Å^3$ associated with the Hf atom. Refinement of the structure with form factors corrected for anomalous dispersion led to the correct assignment of the enantiomer by comparison of the goodness-of-fit ($f'' > 0$ $S = 2.28$; $f'' < 0$ $S = 1.73$). The final cycle of refinement was based on coordinates of the correct enantiomer (and $f'' > 0$); these are given in Table VII. Bond lengths and angles are given in Table VIII.

**Acknowledgment.** The work was supported by the National Science Foundation (Grant CHE 8024869). The use of the Southern California Regional NMR Facility, supported by National Science Foundation Grant CHE 7916324, is also gratefully acknowledged.

**Registry No. 1**, 96866-72-7; **2**, 96866-73-8; **3**, 96866-74-9; **4**, 96866-75-0; **5**, 96866-76-1; **6**, 96866-77-2; **7**, 96866-78-3; **8**, 96866-79-4; **9**, 96866-80-7; **10**, 96866-81-8; **11**, 96896-98-9; **12**, 96866-82-9; $Cp^*HFCl_2\{\eta^2\text{-}^{13}C(O)P(CMe_3)_2\}$, 96866-83-0; $Cp^*HFCl_3$, 75181-08-7; $Cp^*HFMeCl_2$, 96866-84-1; $Cp^*HFMe_2Cl$, 96866-85-2; $Cp^*HFPhCl_2$, 96866-86-3; $Cp^*HFH_2Cl$, 96866-87-4; $HP(CMe_3)_2$, 819-19-2; $LiP(CMe_3)_2$, 19966-86-0; $LiCH_2CMe_3$, 7412-67-1; $KCH_2Ph$, 2785-29-7; $C_2H_4$, 74-85-1; CO, 630-08-0; Hf, 7440-58-6; P, 7723-14-0.

**Supplementary Material Available:** Table IX (Gaussian amplitudes (**7**)), Table X (hydrogen atom coordinates (**7**)), Table XI (listing of structure factor amplitudes (**7**)), $10F_o$, $10F_c$, $10(F_o^2 - F_c^2)/\sigma_{F^2}$ ($F_o < 0$ implies $I_o < 0$), Table XII (Gaussian amplitudes (**12**)), Table XIII (hydrogen atom coordinates (**12**)), and Table XIV (listing of structure factor amplitudes (**12**)) (64 pages). Ordering information is given on any current masthead page.

(52) "International Tables for X-Ray Crystallography"; Kynoch Press: New York, 1974; Vol. IV, pp 72–98.

(53) The data were also corrected for absorption by the method of Gaussian quadrature for the 2120 reflections with multiple observations; the goodness-of-fit decreased from 3.56 to 3.25 with the correction alone (Busing, W. R.; Levy, H. A. *Acta Crystallogr.* **1957**, *10*, 180).